REPORT DOCUMENTATION PAGE

Form Approved OMB NO. 0704-0188

1. REPORT DATE (DD-MM-YYYY)	2. REPORT TYPE	3. DATES COVERED (From - To)
17-11-2009	Final Report	1-Oct-2003 - 30-Sep-2007

4. TITLE AND SUBTITLE
Photonic Synthesis and Processing of Ultrabroadband Radio-Frequency Waveforms

5a. CONTRACT NUMBER
DAAD19-03-1-0275

5b. GRANT NUMBER

5c. PROGRAM ELEMENT NUMBER
611102

6. AUTHORS
Andrew M. Weiner

5d. PROJECT NUMBER

5e. TASK NUMBER

5f. WORK UNIT NUMBER

7. PERFORMING ORGANIZATION NAMES AND ADDRESSES
Purdue University
Sponsored Programs Services
Young Hall, 302 Wood Street
West Lafayette, IN 47907 -2108

8. PERFORMING ORGANIZATION REPORT NUMBER

9. SPONSORING/MONITORING AGENCY NAME(S) AND ADDRESS(ES)
U.S. Army Research Office
P.O. Box 12211
Research Triangle Park, NC 27709-2211

10. SPONSOR/MONITOR'S ACRONYM(S)
ARO

11. SPONSOR/MONITOR'S REPORT NUMBER(S)
45485-EL.10

12. DISTRIBUTION AVAILIBILITY STATEMENT
Approved for Public Release; Distribution Unlimited

13. SUPPLEMENTARY NOTES
The views, opinions and/or findings contained in this report are those of the author(s) and should not contrued as an official Department of the Army position, policy or decision, unless so designated by other documentation.

14. ABSTRACT
The overall objective of this project was to investigate the use of broadband photonic techniques, initially developed in the context of ultrafast optics, for synthesis and processing of ultrabroadband radio-frequency (RF) electromagnetic signals, with an emphasis of signals beyond the speed and bandwidth limits of direct electronic solutions. Although much of the work performed falls into FCC's 3.1-10.6 GHz UWB band, our methods are directly applicable also to higher frequency bands, with results demonstrated up to 50 GHz.

15. SUBJECT TERMS
photonics; radio-frequency; arbitrary waveform generation

16. SECURITY CLASSIFICATION OF:			17. LIMITATION OF ABSTRACT	15. NUMBER OF PAGES	19a. NAME OF RESPONSIBLE PERSON
a. REPORT	b. ABSTRACT	c. THIS PAGE			Andrew Weiner
UU	UU	UU	UU		19b. TELEPHONE NUMBER: 765-494-5574

5 **Photonic Time-Domain Electromagnetic Signal Generator and System Using the Same**

Patent Filed in US? (5d-1) Y

Patent Filed in Foreign Countries? (5d-2) N

Was the assignment forwarded to the contracting officer? (5e) N

Foreign Countries of application (5g-2):

5a: Jason D. McKinney

5f-1a: Purdue University

5f-c:

West Lafayette IN 47907

5a: Andrew M. Weiner

5f-1a: Purdue University

5f-c:

West Lafayette IN 47907

1. Introduction

The overall objective of this project was to investigate the use of broadband photonic techniques, initially developed in the context of ultrafast optics, for synthesis and processing of ultrabroadband radio-frequency (RF) electromagnetic signals, with an emphasis of signals beyond the speed and bandwidth limits of direct electronic solutions. Although much of the work performed falls into FCC's 3.1-10.6 GHz ultrawide (UWB) band, our methods are directly applicable also to higher frequency bands, with results demonstrated up to 50 GHz.

This project has succeeded in photonic synthesis of a variety of ultrawideband-applicable signals including monocycle and impulsive waveforms and has introduced and demonstrated the concept of spectral engineering, in which the bandwidth, and center frequency of arbitrary impulsive RF waveforms is tailored through waveform design. This allows realization of electrical waveforms with spectra close to flat within the 3.1-10.6 GHz band. This project has also exploited photonic waveform synthesis capabilities to compensate for phase distortions in broadband antennae, resulting in substantial compression of received signals, including significant enhancement of received signal amplitudes. These experiments are the first of their kind for RF signals spanning bandwidths of order 10 GHz.

A note on terminology: this report uses the term "ultrabroadband" to refer to pulsed RF signals with center frequencies in the GHz to many tens of GHz range, very large fractional bandwidths, and very large instantaneous bandwidths. This is similar to the common term "ultrawideband (UWB)," which however is now taking on a more specific meaning due to Feb. 2002 rulings by the FCC, which allows UWB operation in the 3.1-10.6 GHz band [1]. Here the term "ultrabroadband" is used not only to include UWB as defined by the FCC ruling but also more generally to allow other frequencies or higher frequencies as well.

2. Ultrabroadband radio-frequency arbitrary waveform generation

Figure 1(a) illustrates a concept for photonic synthesis of arbitrary burst RF waveforms which we first demonstrated under a preceding grant from ARO (DAAD19-00-1-0497). The idea is to exploit our well developed optical pulse shaping technology [2]. An ultrashort input pulse is first shaped as desired, then directed to a fast optical-to-electrical converter (O/E). By controlling the optical excitation waveform onto the O/E, cycle-by-cycle synthesis of burst RF waveforms can be achieved.

Under DAAD19-00-1-0497 we demonstrated this approach in the mm-wave region [3]. An example of data measured using a 50 GHz sampling oscilloscope is shown in Fig. 1(b). Here the optical pulse shaper is set to generate a series of three optical pulses with ~21 ps spacing, followed by two optical pulse pairs with ~42 ps between pairs. The timing of the optical pulse sequence combined with the low-pass response of the electrical system yields a mm-wave frequency modulation waveform, with three cycles at ~48 GHz switching abruptly to two cycles at ~24 GHz. We have also generated burst waveforms at 48 GHz with abrupt internal phase shifts (Fig. 1(c)).

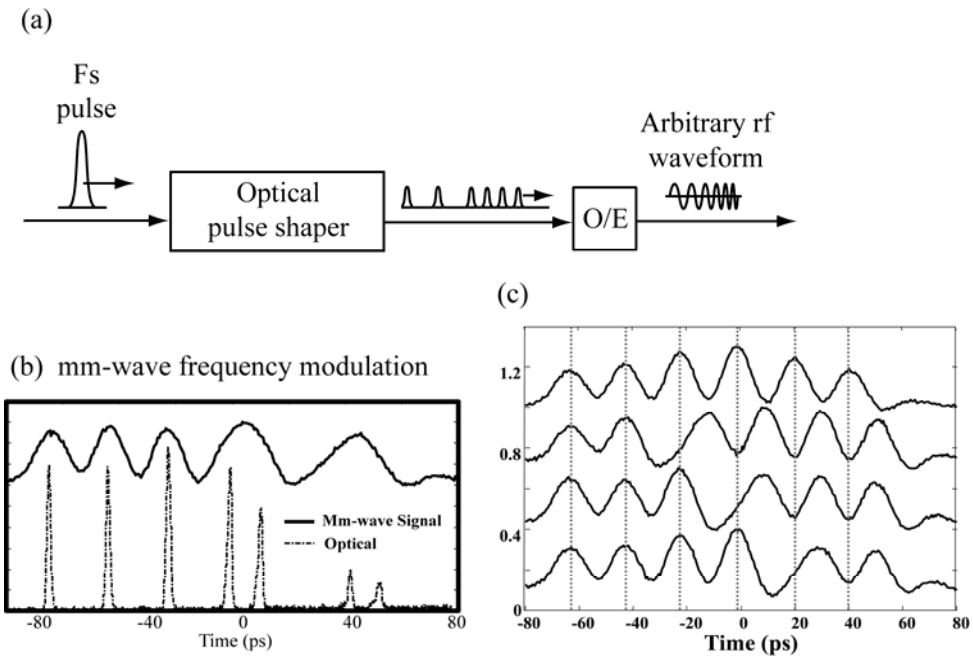

Fig. 1. (a) Setup for photonic generation of arbitrary RF waveforms; (b) Abrupt frequency modulation in the mm-wave region. (c) 48-GHz waveforms with abrupt internal phase modulation.

This work is the first of its kind. Commercial electronic arbitrary waveform generators were limited to bandwidths of 1-2 GHz at the time the current project was initiated, and now (~2009) reach 9.6 GHz at 6 dB bandwidth. The strongly phase- and frequency-modulated voltage waveforms shown in Fig. 1, with center frequencies in the mm-wave regime, could not be generated with any present direct electronic approaches.

One limit of the direct optical pulse shaping approach of Fig. 1(a) involves the time aperture: it is difficult to generate optical waveforms with a time aperture significantly exceeding ~100-200 ps. For burst RF waveforms consisting of at least a few RF cycles, a 100-200 ps time aperture limits this approach to RF frequencies that are tens of GHz and above. Therefore, this approach cannot provide arbitrary waveform generation for RF frequencies in the several-GHz range (e.g., the 3-10 GHz frequency range important for UWB), which is still just barely accessible via the most advanced electronic approaches. Furthermore, even in the low GHz bands now covered by electronic arbitrary waveform generators, the timing jitter of such electronic solutions is high. Photonics offers the unique possibility of ultrabroadband arbitrary waveform generation with low timing jitter, which is important for a number of applications.

In order to smoothly extend the photonic approach to reach into the low frequency at the edge of electronics capabilities, in the current project we used the stretched pulse approach shown in Fig. 2. [4,5]. Here the pulse shaper acts as an arbitrary optical spectral filter, allowing generation of broadband optical signals with power spectra structured according to specification. The spectrally filtered optical signal passes through a dispersive stretcher (e.g., a few km of optical fiber), which stretches the signal to yield a time aperture up to tens of nanoseconds. The optical output waveform in time is approximately equal to a scaled version of the optical power

spectrum. Spatial light modulators that can be used in pulse shaping can comprise 100 (perhaps up to ~1000) individually controllable pixels, which means stretched optical waveforms with time-bandwidth products in the range 100-1000 should be possible. After converting to RF using an appropriate photodetector, it becomes possible to obtain burst microwave signals with center frequencies in the several GHz range, 100% fractional bandwidth, time apertures of nanoseconds (extendible to tens of nanoseconds), and large time-bandwidth products with user-specified modulation.

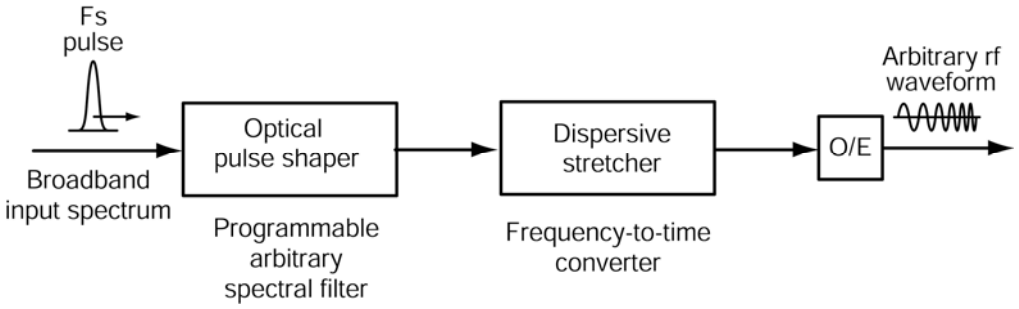

Fig. 2. Concept for microwave arbitrary waveform generation exploiting time stretching.

We have succeeded in generating a variety of ultrabroadband RF waveforms using this approach [4]. In Figure 3, the optical spectrum is shaped to give an RF waveform that is discretely frequency-modulated from 1.25 – 2.5 – 5 GHz over a time aperture of ~ 1.75 ns, as shown in (a). In 3(b) the measured RF spectrum (linear scale) clearly shows spectral peaks at 1.25, 2.5, and 5 GHz.

We have also considered broadband monocycle and impulsive waveforms. Such waveforms, exhibiting temporal features on the order of ~100 ps, have extremely large instantaneous bandwidth and are, thus, appealing for applications such as ultrawideband communication, imaging, and radar applications. Electrical UWB systems tend to emphasize the use of ‘zero-area’ electrical monocycles to achieve the large RF bandwidths. The limitations of electrical techniques, however, include limited pulse-rate and fixed pulse shapes. In our work we’ve demonstrated monocycle burst waveforms exhibiting monocycle durations shorter than those that were achievable with purely electronic techniques, as well as polarity reversals and variable delay between monocycles. An example monocycle burst is shown in Figure 4(a). Here, monocycle durations are on the order of 200 ps, although our method allows much shorter durations if desired. Additionally, the center monocycle shows a polarity reversal – such reversals are often difficult to achieve using electronic techniques given the fixed electronic pulse shaping networks used to generated monocycle waveforms. Finally, the delay between adjacent monocycles is tunable; here we demonstrate a monocycle spacing that varies from ~1ns between the first two cycles to ~500 ps between the second and third cycles. From Fig. 4(b) this waveform is seen to be extremely broadband with non-zero spectral content ranging from DC to approximately 8 GHz.

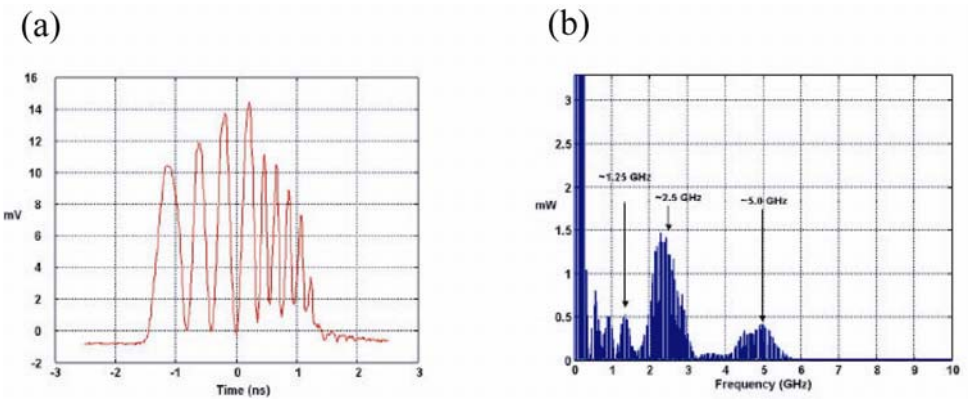

Fig. 3. (a) Frequency stepped RF waveform showing distinct cycles at 1.25 GHz, 2.5 GHz, and 5 GHz. (b) RF power spectrum of frequency stepped waveform.

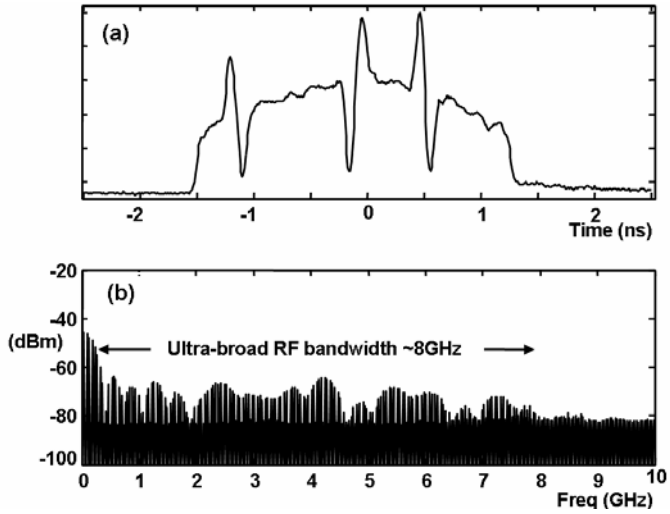

Figure 4 – (a) Monocycle burst waveform. Here, we demonstrate monocycle durations of ~200 ps, arbitrary polarity reversals, and variable delay on a scale not achievable via electronic techniques. (b) RF power spectrum exhibiting an ~8 GHz bandwidth.

4. Spectral Engineering

With reference to the FCC UWB transmission band, maximum power spectral density limits are specified both in and out of the 3.1-10.6 GHz band. In order to transmit the maximum allowable pulse *energy*, one needs to generate a transmit-waveform that is maximally flat in the allowed band. Although time-hop sequences often used for UWB communications can be designed to shape the overall spectrum [6], there are constraints, especially if one is relying on time hopping for other reasons, such as multi-access. A similar concept applies in chirped radar, where transmit signals are stretched in time to achieve required transmit energies at limited peak power, while frequency modulation is used to provide bandwidth and hence range resolution. Photonic RF arbitrary waveform generation can serve as a new tool for optimally shaping

transmitted power spectra in a variety of RF systems [7]. This will be especially useful in cases where the power spectral density function is constrained.

To illustrate the concept of spectral engineering, consider the baseband impulsive waveform of Figure 5(a) and corresponding RF power spectrum of Fig. 5(b). Here, we numerically define the target RF power spectrum to be a super-Gaussian with spectral width from 0 to 4 GHz. The desired time-domain waveform is then achieved via a numerical fast-Fourier transform. The resulting shape is then applied to the optical power spectrum in our system. The measured electrical waveform of Fig. 5(a) results. This baseband impulsive waveform (main peak ~100 ps) yields the measured ~4 GHz spectrum shown in Fig. 5(b). Though the spectrum exhibits the desired 4 GHz bandwidth, there is significant ripple apparent from DC to approximately 2 GHz. This ripple arises from the steep rising / falling edges of the time domain waveform, which is due to the sharp truncation of the optical power spectrum in the pulse shaper. Since our system relies on shaping of the optical intensity, there is fundamentally an unavoidable DC component; however, the ripple in Fig. 5(b) may be minimized through proper apodization of the time domain waveform.

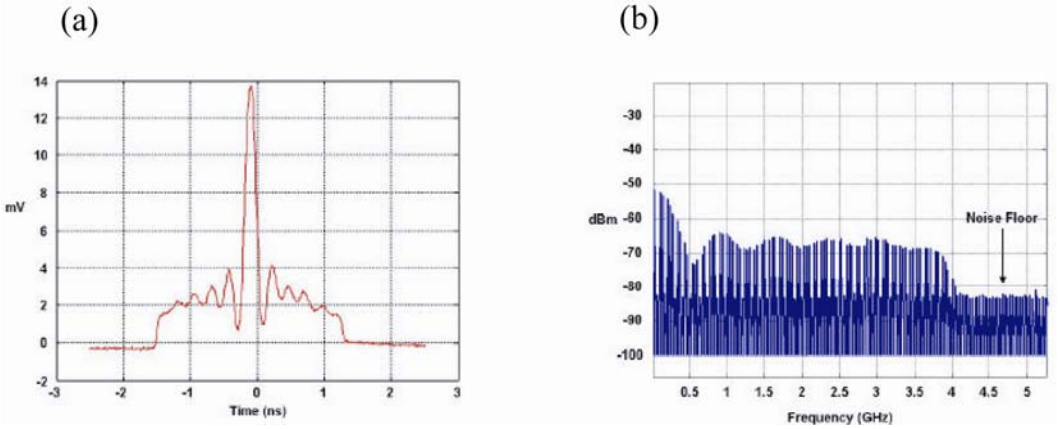

Fig. 5. (a) Impulsive waveform superimposed on modulation structure intentionally designed to flatten power spectrum. (c) Measured RF power spectrum, close to flat over nearly 3 GHz band.

Figure 6(a) – (c) further illustrates this concept as well as the ability to tune the center frequency of our waveforms. Here, an impulsive waveform is designed in much the same way as above. The exception is that the target RF spectrum is centered at 4 GHz and the desired time-domain waveform is multiplied by a ~1 ns Gaussian apodization waveform. The shaped optical spectrum is shown in Fig. 6(a) and the resulting time-domain waveform is shown in Fig. 6(b) – note the close resemblance as expected in our frequency-to-time conversion approach. Here, the steep rising / falling edges have been replaced with a smoothly varying Gaussian envelope. In the frequency domain, the result is a 4 GHz-wide super-Gaussian spectrum centered at ~4 GHz that shows significantly reduced ripple. The frequency null in the ~500 MHz – 2 GHz region clearly shows the result of modulation and apodization of the time-domain waveform. Such ability to zero spectral content in a given frequency band is required, for example, in UWB systems specified to operate in the 3.1 – 10.6 GHz frequency range.

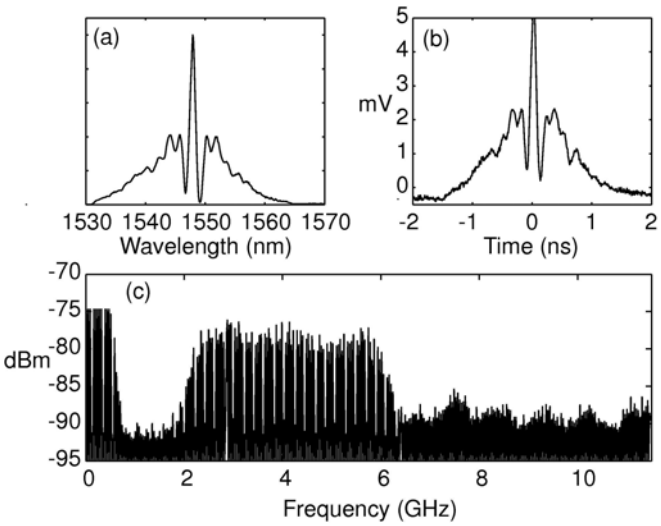

Figure 6 – Impulsive waveform synthesized via spectral engineering. Here, the bandwidth and center frequency are chosen to be 4 GHz. (a) Shaped optical power spectrum. (b) Time-domain waveform. (c) RF power spectrum showing the effects of modulation and apodization of the time-domain waveform - reduced ripple and zero frequency content from ~500 MHz – 2 GHz.

The concept of spectral engineering – namely the ability to define the shape, bandwidth, and center frequency of a particular waveform – is extensible to waveforms spanning the entire UWB band [7]. A waveform illustrating this potential is shown in Figure 7. The time-domain RF waveform in Fig. 7(a) is similar to that shown in Fig. 6, except with shorter impulse and fast surrounding modulation. The details are chosen to realize a spectrum that is centered in and nearly spans the UWB band, with 115% fractional bandwidth and ripple below ±1.4 dB in the range 4-9 GHz. Even with the most modern electronic instruments, generation of such spectra is extremely difficult.

For situations in which only the power spectrum is of interest, the frequency dependent phase remains unconstrained. This means that there are many different time domain waveforms that can furnish the same power spectrum. For example, instead of the impulsive waveforms of Figs. 5 and 6, we can use frequency swept (chirp) signals. Figure 8 shows an example, in which the signal is swept over the UWB band in approximately 1 nanosecond. Although the drive waveform is not fully optimized, the spectrum remains flat over the same 4-9 GHz range (now within ±2.8 dB). Meanwhile, with peak voltage remaining approximately the same, the power spectral density of the generated waveform increases by 8 dB. For a peak power limited system, this concept allows increased waveform energy by spreading the time aperture of the generated signal while maintaining bandwidth. This concept is similar to the well known principle of chirped radar, but extended to much larger fractional bandwidths than usual systems.

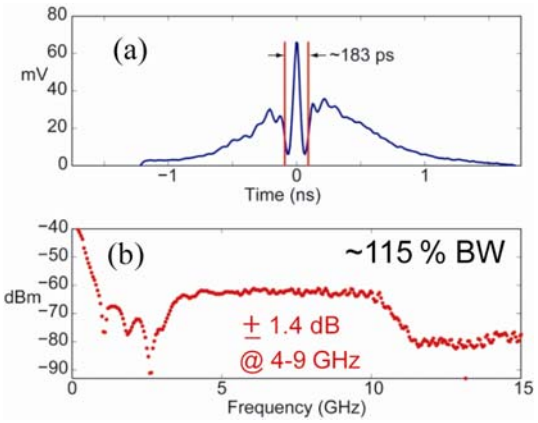

Fig 7. Impulsive waveform (a) designed to give nearly flat power spectrum (b) over the UWB band.

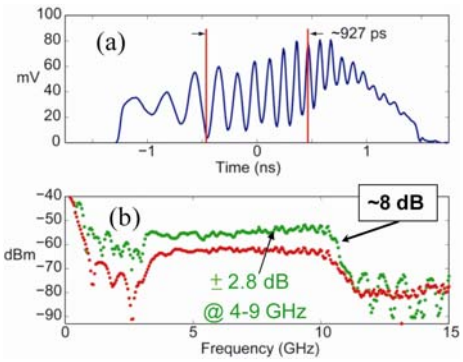

Fig. 8. Frequency modulated (chirped) waveform (a) designed to give nearly flat power spectrum (b, green curve) over the UWB band. The power spectrum using the impulsive waveform of Fig. 7 is potted for reference (red curve). The frequency-modulated waveform provides 8 dB increase in power spectral density.

5. Antenna Dispersion Compensation

In moving our RF-AWG technique and apparatus towards applications in wireless RF systems, we have begun to investigate the effects of broadband antennae on impulsive UWB signals. Given the broad frequency bandwidth available to UWB wireless systems, it is desirable for the antennae in these systems to exhibit an ideal frequency response over the 3.1 - 10.6 GHz UWB frequency band. Such an idealized response - consisting of a flat frequency response and linear phase delay - is, functionally, rarely achieved as broadband antennae are not generally designed with RF phase considerations in mind. The result is that, when a broadband antenna is impulsively excited, the voltage received by a second antenna is dispersed in time due to the nonlinear RF spectral phase response of the transmit antenna. This phenomena is easily observed in UWB systems, and the concept of precompensating the transmit waveforms in these systems to compress the received voltage waveform has been the subject of significant theoretical work [8]. To our knowledge, however, prior to the work reported here, there have been no experimental demonstrations of this concept.

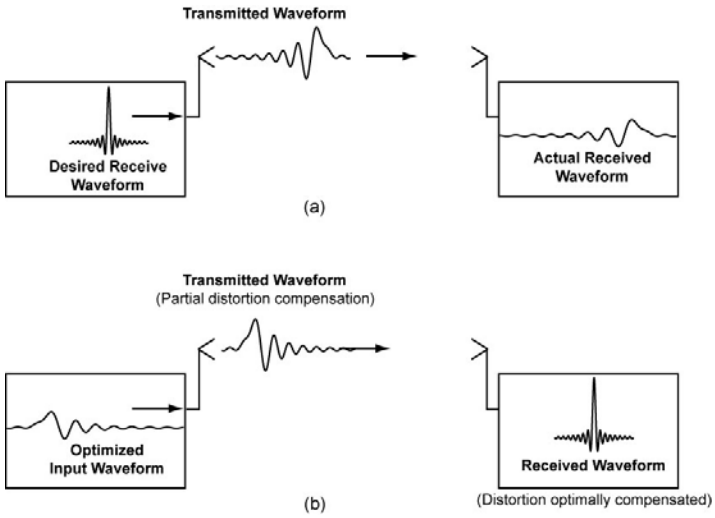

Fig. 9 – Schematic of antenna distortion compensation concept. (a) When an impulse is transmitted, the received waveform is distorted due to the phase velocity and amplitude transmission function of the antennae. (b) By transmitting a tailored waveform (time-reversed, e.g.), the received waveform is recompressed.

Our concept is shown schematically in Figure 9. First, an impulsive drive signal is used to excite the transmit antenna, and the waveform received via a second antenna is measured. By using this measured impulse response to predict the received waveform based on a particular input, we aim to optimize the received signal (e.g., minimize the received signal duration) through tailoring of the input waveform. As a first demonstration of this concept, we now apply a time-reversed version of the impulse response to the transmit antenna. Practically, this should serve to 'undo' the phase distortion arising from the frequency-dependent propagation velocity in the antenna pair and recompose the pulse.

Figure 10 shows a schematic of the experimental apparatus used for these antenna experiments [9]. Arbitrary RF waveforms from our apparatus are used as the excitation for a commercial, broadband ridged TEM horn antenna. A second identical antenna, positioned ~1 meter away, functions as a receiver, and the output of this antenna is measured on a 50 GHz sampling oscilloscope. When the ~400 mV (peak) ~18 ps impulse of Figure 11(a) (inset) is applied to the transmit antenna, the received waveform (Fig. 11(b)) is observed to have a duration of ~4 ns and clearly exhibits dispersion; the waveform consists of a monocycle that contains the high-frequency content of the driving impulse, followed by a low frequency ringing (~1 GHz). Here, the dispersion between the low (~1 GHz) and high (~14 GHz) frequency components of the waveform is attributed to the significant RF spectral phase variations near the cutoff frequencies of the transmit antenna.

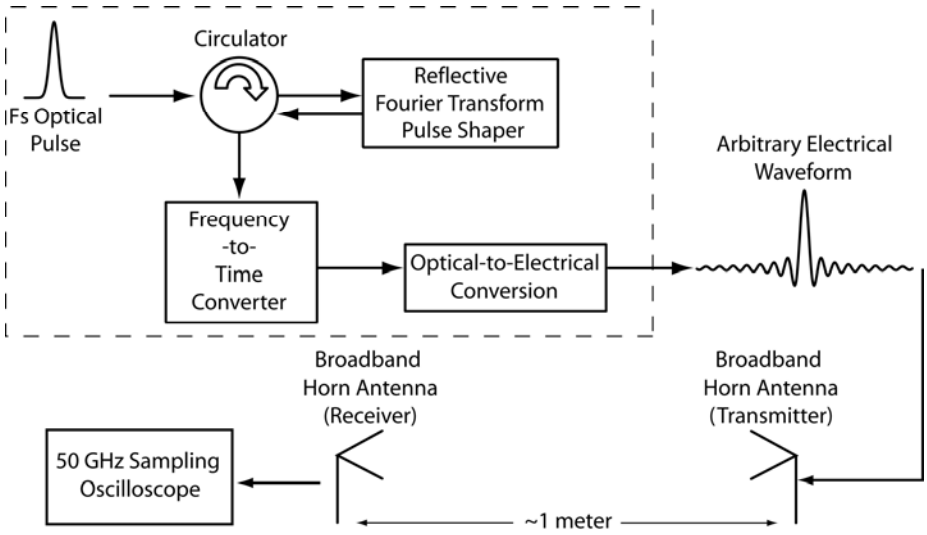

Fig. 10 – Experimental apparatus for broadband antenna phase-compensation experiments.

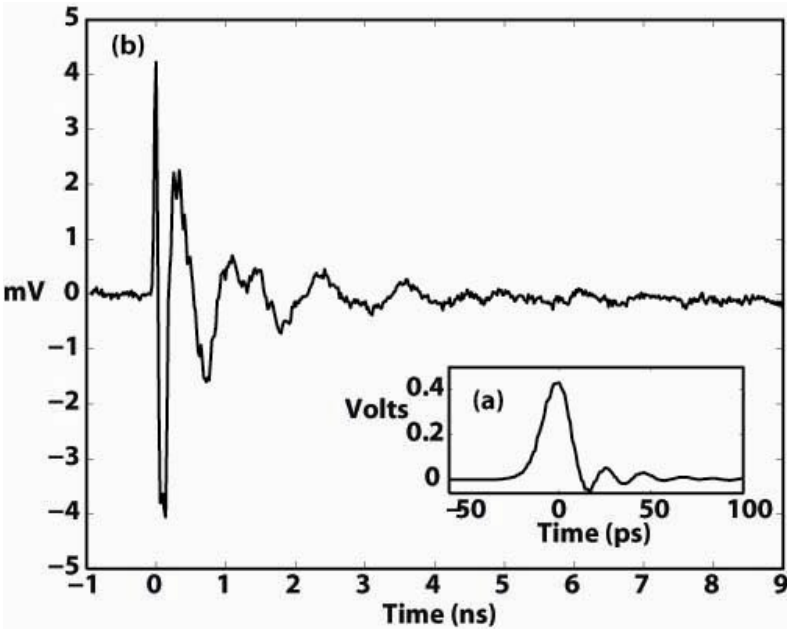

Fig. 11 – (a) ~18 ps impulsive excitation waveform applied to the transmit antenna. (b) Measured impulse response of the antenna link clearly exhibiting the dispersion induced by the broadband antennae.

The frequency content of the impulse of Fig. 1(a) (up to approximately 25 GHz) far exceeds the specified bandwidth of our antennae (~1 – 12 GHz). Thus, the waveform of Fig. 11(b) is effectively the impulse response of the antenna link. By extracting the RF spectral phase obtained via Fast-Fourier Transform of the impulse response, we are then able to design an input waveform exhibiting the opposite spectral phase response, i.e, a time-reversed version of the impulse response. This is effectively the matched filter solution to the antenna link. To obtain an approximation to this matched signal, the antenna link impulse response is sampled and a time-reversed version of the sampled waveform is applied as the optical filter function in our RFAWG

apparatus. Figure 12 shows the measured approximation to the time reversed impulse response synthesized in our system. It should be noted that, given the approximately 3 ns time aperture of our RF-AWG system, we are motivated to choose the first ~3ns of the impulse response in order to capture the majority of the high-frequency content of the signal. It should be noted that this waveform exhibits a peak voltage of approximately 35 mV (over an order of magnitude smaller than the impulse of Fig. 11(a).)

Figure 13 shows the measured received waveform when the signal of Fig. 12 excites the transmit antenna. Here the received waveform exhibits a single central peak preceded and followed by several low amplitude secondary oscillations. Though the excitation waveform is only an approximation to the matched excitation signal, the received voltage waveform is clearly compressed. Three metrics that can be used to quantify this compression are the received waveform duration, the peak received voltage value (relative to that of the input), and the amplitude of the secondary oscillations (sidelobes) relative to the amplitude of the largest peak in the received waveform. Here, we consider these metrics with respect to the normalized power of the received waveforms. We define the normalized power as the magnitude-squared of the received voltage divided by the peak magnitude-squared voltage of the excitation waveform. The normalized power of the received waveform under impulsive and ‘’matched’’ excitation is shown in Figures 14 and 15, respectively.

For our experiments, we define the waveform duration as the time interval over which any oscillations reach 50 % of the peak normalized power in the received waveform. The 84.6 ps duration exhibited by the ‘’matched’’ received waveform is approximately 2x shorter than the 174 ps duration of the measured antenna link impulse response. In terms of the peak received voltage, the peak voltage level in the received waveform (Fig. 13, Vpk~2 mV) is only ~ 2x smaller than the peak received voltage under impulsive excitation (Fig. 11(b), Vpk~4 mV). The exciting impulse, however, has over a 10x larger peak voltage than the approximate ‘’matched’’ excitation waveform. The peak normalized power under ‘’matched’’excitation is then found to be 36-times larger than that resulting from impulsive excitation This clearly shows the received voltage under ‘’matched’’ excitation is compressed as compared to the case of purely impulsive excitation. Another (potentially more insightful) metric to describe compression of the received waveform – or, alternatively, how well a particular signal and system are matched - is the level of the secondary oscillations relative to that of the main signal peak. This is analogous to comparing the power in the main beam of an antenna array to the power in the sidelobes. We define the sidelobe level for our signals to be

$$S = 10\ \log_{10} \frac{|V_n|^2}{|V_p|^2},\ \text{(dB)}$$

where $|V_n|$ is the voltage magnitude of the n-th secondary oscillation and $|V_p|$ is the voltage magnitude of the largest oscillation. Table 1 summarizes this comparison. Comparison of the measured sidelobe levels for the “matched” signal with those of the impulse response shows a dramatic improvement. Though the experimental input “matched” signal is only an approximation to the ideal matched signal, the n = 1 oscillation in the matched response has been pushed down to approximately the level of the n = 3 sidelobe in the impulse response; all other

oscillations in the matched response have been pushed well below the n = 3 sidelobe in the impulse response.

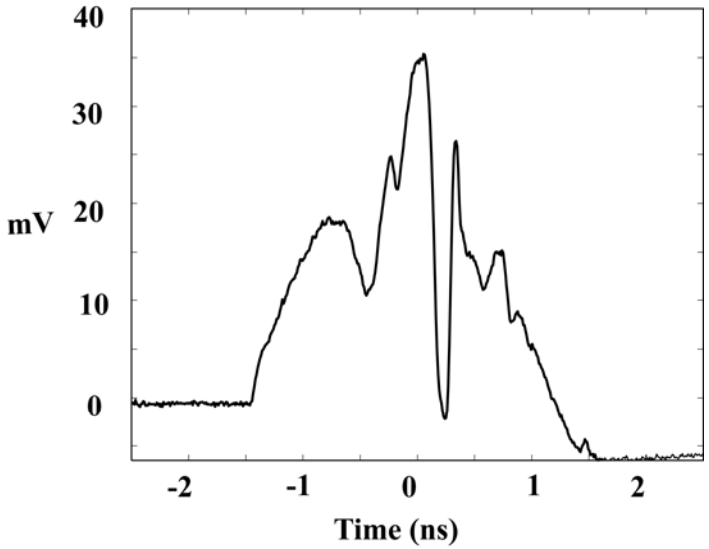

Fig. 12 – Measured approximation to the matched signal for our antenna link as synthesized in our RFAWG apparatus.

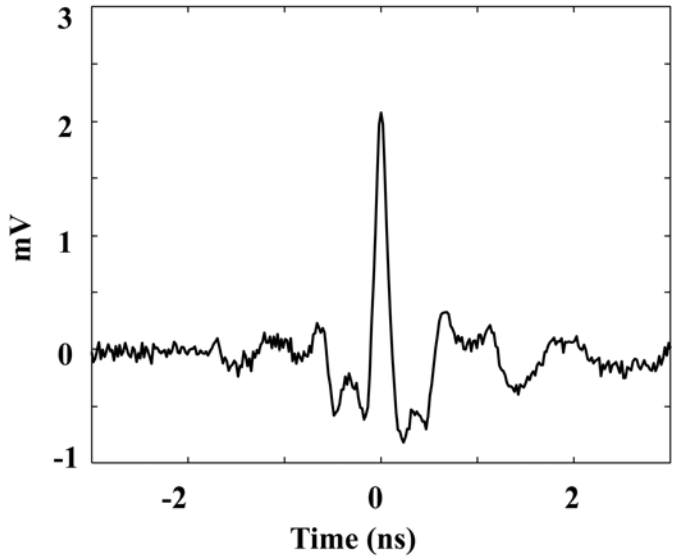

Fig. 13 – Received waveform for the case of approximately matched excitation.

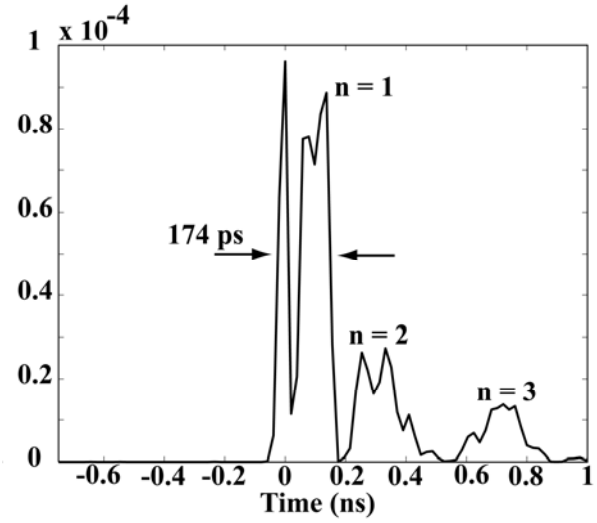

Fig. 14 – Normalized power of the impulse response of the antenna link.

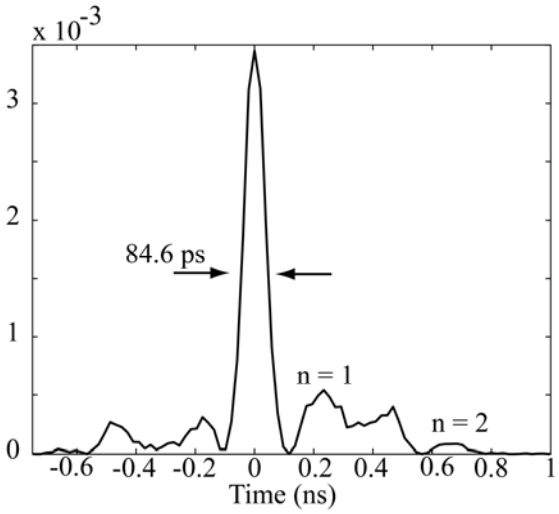

Fig. 15 – Normalized power of the received signal of the antenna link response under "matched" excitation.

Table 1 – Comparison of sidelobe levels for impulsive and matched excitation

Signal	Sidelobe #	Position (ns)	S (dB)
Matched	n = -2	-0.5	-11.1
	n = -1	-0.18	-10.5
	n = 1	0.23	-8.1
	n = 2	0.68	-16.1
Impulse	n = 1	0.135	-0.3
	n = 2	0.331	-5.4
	n = 3	0.71	-8.5

We have performed a number of further experiments, in which we exploit photonically enabled RF arbitrary waveform generation to measure and compensate the dispersion of broadband, line-of-sight antenna links [10,11]. In addition to the horn antennas discussed above, we have also investigated log-periodic and spiral antennas, and links consisting of two identical antennas as well as links where different types of antennas are used for transmitting. As an example, Figures 16 and 17 show data for the case of log-periodic transmitter antenna coupled via line-of-sight to a horn antenna receiver. Figure 16 shows the impulse response measured using a 20 ps laser generated voltage pulse for excitation. The received signal is stretched by nearly a factor of 300 to 5.7 ns, with a frequency sweep (from high to low frequencies) clearly visible. Figure 17 shows the dispersion compensation results for experiments in which the bandwidth is chosen to support an ~200 ps electrical impulse. The top row shows impulse results: a 195 ps electrical input (left) is broadened by more than a factor of ten to 2.17 ns (middle). The bottom row shows the case where the electrical input waveform (left) is chosen according to be a time-reversed version of the impulse response. The received waveform (middle) is now compressed to 264 ps, close to the bandwidth-limit. Thus, more than a factor of ten pulse compression is achieved. The normalized power plots (right column) highlight the dramatic compression of the received waveform, as well as a factor of 17 enhancement in normalized power that accompanies compression.

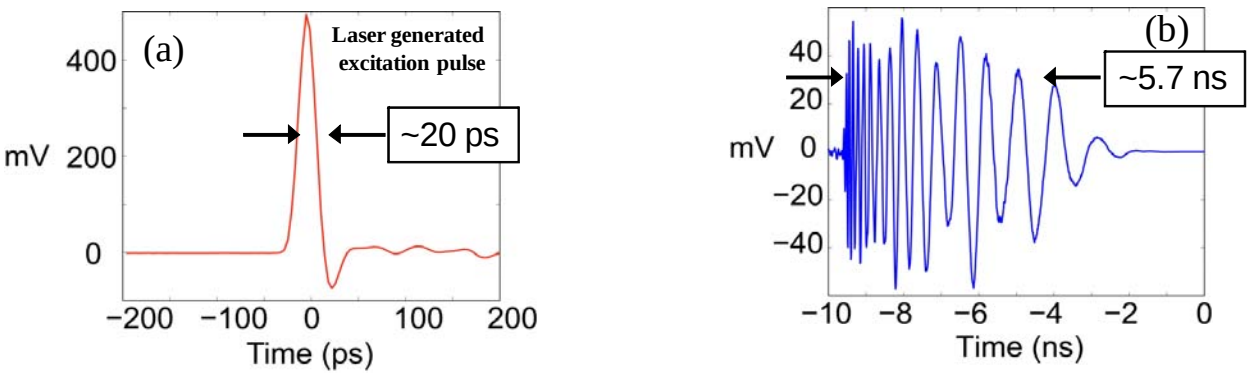

Fig. 16. Impulse response measurement of line-of-sight log periodic antenna-horn antenna link (a) 20 ps excitation pulse. (b) Received waveform.

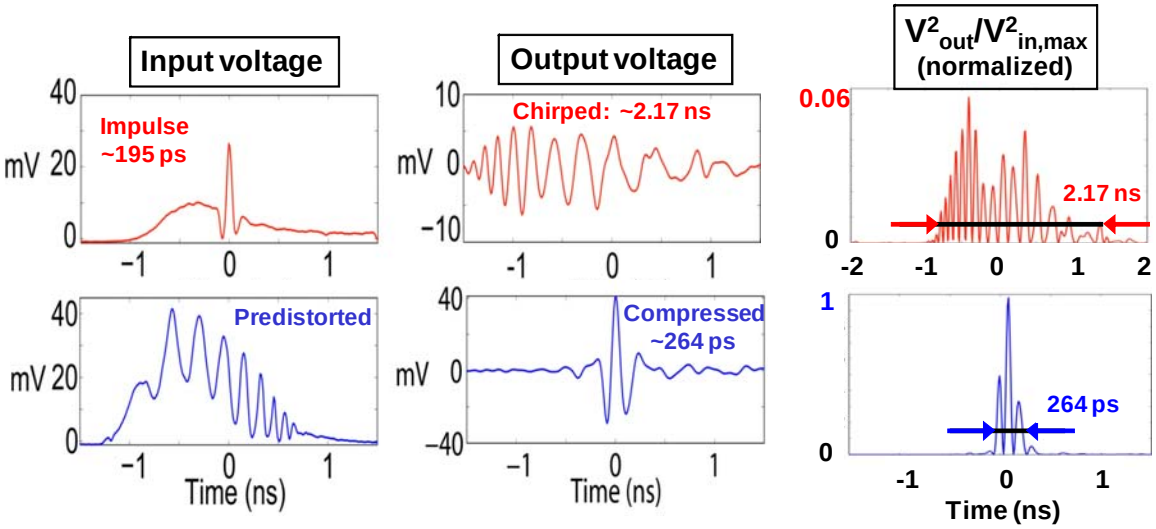

Fig. 17. Experiments with log periodic antenna-horn antenna link. (top row) Experiments with ~195 ps impulses. (bottom row) Experiments with time-reversed impulse response used for excitation, resulting in compressed output pulses.

These experiments illustrate new capabilities that become possible with ultrabroadband radio-frequency waveform control, enabled here by high-speed photonics technologies. Such waveform generation capability may contribute to new concepts for ultrabroadband radar, radio-frequency sensing, wireless communications and electronic warfare.

References

1. "First report and order (revision of part 15 of the Comission's rules regarding ultra-wideband transmission systems)," FCC, Washington, DC, eT Docket 98-153, adopted February 14, 2002, released April 22, 2002.
2. A.M. Weiner, "Femtosecond Pulse Shaping Using Spatial Light Modulators," Rev. Sci. Instr. **71,** 1929-1960 (2000).
3. J.D. McKinney, D.E. Leaird, and A.M. Weiner, "Millimeter-Wave Arbitrary Waveform Generation with a Direct Space-to-Time Pulse Shaper," Opt. Lett. **27,** 1345-1347 (2002).
4. I. S. Lin, J. D. McKinney, and A. M. Weiner, "Photonic synthesis of broadband microwave arbitrary waveforms applicable to ultra-wideband communication," *IEEE Microw. Wireless Compon. Lett.*, vol. 15, no. 4, pp. 226–228, Apr. 2005.
5. J. Chou, Y. Han, and B. Jalali, "Adaptive RF-photonic arbitrary waveform generator," *IEEE Photon. Technol. Lett.*, vol. 15, no. 4, 581-583, Apr. 2003.
6. M.Z. Win and R.A. Scholtz, "Impulse Radio: How It Works," IEEE Communications Letters **2,** 36-38 (1998).
7. J. D. McKinney, I. S. Lin, and A. M. Weiner, "Shaping the power spectrum of ultrawideband radio-frequency signals," *IEEE Trans. Microw. Theory Tech.*, vol. 54, no. 12, pp. 4247-4255, Dec. 2006.
8. D. M. Pozar, "Waveform optimizations for ultrawideband radio systems," *IEEE Trans. Antennas Propag.*, vol. 51, no. 9, pp. 2335-2345, Sep. 2003.
9. J. D. McKinney, and A. M. Weiner," Compensation of the effects of antenna dispersion on UWB waveforms via optical pulse-shaping techniques," *IEEE Trans. Microw. Theory Tech.*, vol. 54, no. 4, pp. 1681-1686, Apr. 2006.
10. J. D. McKinney, D. Peroulis, and A. M. Weiner, "Dispersion limitations of ultrawideband wireless links and their compensation via photonically enabled arbitrary waveform generation," *IEEE Trans. Microw. Theory Tech.*, vol. 56, no. 3, pp. 710-719, Mar. 2008.
11. J. D. McKinney, D. Peroulis, and A. M. Weiner, "Time-domain measurement of the frequency-dependent delay of broadband antennas," *IEEE Trans. Antennas Propagat.*, vol. 56, no. 1, pp. 39-47, Jan 2008.